

RSC Advances



This is an *Accepted Manuscript*, which has been through the Royal Society of Chemistry peer review process and has been accepted for publication.

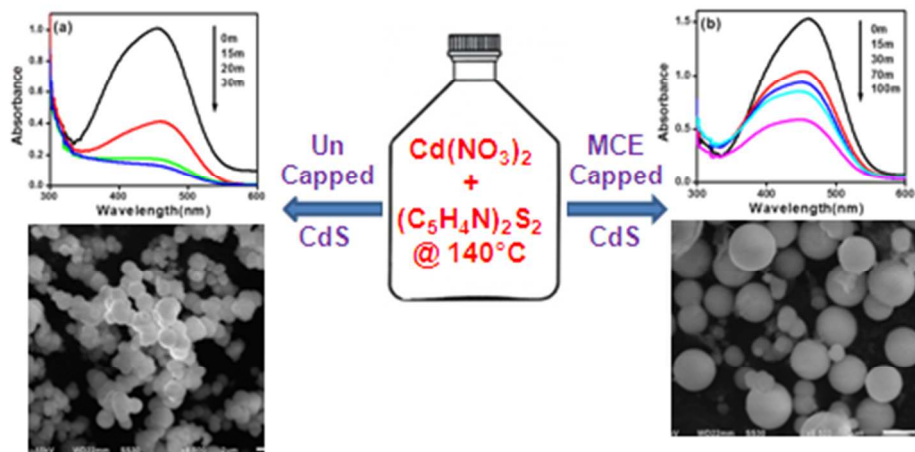
Accepted Manuscripts are published online shortly after acceptance, before technical editing, formatting and proof reading. Using this free service, authors can make their results available to the community, in citable form, before we publish the edited article. This *Accepted Manuscript* will be replaced by the edited, formatted and paginated article as soon as this is available.

You can find more information about *Accepted Manuscripts* in the [Information for Authors](#).

Please note that technical editing may introduce minor changes to the text and/or graphics, which may alter content. The journal's standard [Terms & Conditions](#) and the [Ethical guidelines](#) still apply. In no event shall the Royal Society of Chemistry be held responsible for any errors or omissions in this *Accepted Manuscript* or any consequences arising from the use of any information it contains.

For graphical abstract

A one-pot, template-free, solvothermal method for synthesizing CdS microspheres composed of ultrasmall (~ 2 nm) nanocrystals using $(C_5H_4N_2)S_2$ as in situ source of S^{2-} ions without and with the use of MCE-capping agent has been developed. The photocatalytic activity of the microspheres for degradation of MO under UV and natural sunlight irradiation has been compared.



Template-free Syntheses of CdS Microspheres Composed of Ultrasmall Nanocrystals and their Photocatalytic Study

Manjodh Kaur and C. M. Nagaraja*

Department of Chemistry, Indian Institute of Technology Ropar, Rupnagar 140001, Punjab, India. Tel:+91-1881242229, **Email:** cmnraja@iitrpr.ac.in

Abstract

Template-free CdS microspheres composed of nanocrystals have been successfully synthesized by a one-pot solvothermal method using 4,4'-dipyridyldisulfide (DPDS = $(C_5H_4N)_2S_2$) as a temperature controlled in situ source of S^{2-} ions without (**S1-S3**) and with the use of capping agent (**S4**). The powder X-ray diffraction measurements of all the four (**S1-S4**) samples revealed the cubic structure of the CdS microspheres and SEM analyses showed almost spherical morphology of the CdS microspheres with a broad size range of 0.5 to 2 μm . TEM analyses of the samples **S3** and **S4** revealed that the CdS microspheres are composed with assembled CdS nanocrystals of ultrasmall (2-5 nm) size. Optical investigation of the samples (**S1-S4**) showed blue-shift in the UV-vis absorption maxima compared to that of bulk CdS due to quantum confinement effect. Photocatalytic investigation of the uncapped (**S3**) and mercaptoethanol (MCE)-capped (**S4**) CdS microspheres for degradation of methyloange (MO) revealed that the rate of photocatalytic activity of **S3** is much higher than that of **S4** under both UV and natural sunlight irradiation. The relatively lower activity of **S4** has been attributed due to the presence of MCE capping agents which acts as a barrier for the interaction of MO molecules with the CdS nanocrystals. The proposed mechanism for the formation of CdS microspheres and their photocatalytic activity has also been presented.

1. Introduction

Ultra small semiconducting nanocrystals with the diameter of about 2 nm are attracting increasing current attention due to their size dependent unique optical, electrical, catalytic properties.¹⁻¹⁰ Among the various semiconductor nanomaterials, CdS with a direct band gap of 2.42 eV as attracted much attention due to its diverse applications in photodetectors¹¹, light emitting diodes,¹² solar cells,¹³ photocatalysis¹⁴ and so on. It has been well established that the properties of nanomaterials depend on their crystallite's size, morphology and structure.¹⁵ Therefore, controlling the size and morphology of nanomaterials is crucial for modifying their properties. In this context, extensive efforts have been made by researchers to control the size, shape and morphology of CdS nanomaterials and a variety of morphologies, such as, spheres,¹⁶ rods,¹⁷ triangles,¹⁸ hexagons,¹⁹ etc., have been reported. Literature survey revealed that the formation of these morphologies has been mostly driven by self-assembly processes and assisted by surfactant molecules/capping agents.²⁰⁻²³ On the contrary, it is quite challenging to develop template or capping agent-free routes for the preparation of CdS nanostructures with controlled morphologies.

Syntheses of CdS nanostructures have been reported by using variety of organosulfur compounds, such as, thiourea, thioacetamide, L-Cysteine, etc., as in situ source of S²⁻ ions.^{20, 24-25} We have been attempting to prepare CdS nanostructures with controlled morphology by adopting controllable synthetic reactions at appropriate temperature without the use of surfactant or template molecule. In this context, we recently demonstrated the controlled synthesis and photocatalytic activity of CdS microspheres composed of CdS nanocrystals by employing 4,4'-dipyridyldisulfide (DPDS = (C₅H₄N)₂S₂) as a temperature controlled in situ source of S²⁻ ions without the use of surfactant/template molecule.²⁶ In continuation of our efforts to synthesize template-free, CdS nanostructures, here, we present the syntheses, characterization and photocatalytic activity of CdS microspheres composed of ultrasmall (~ 2 nm) CdS nanocrystals prepared by using DPDS as temperature controlled in situ source of S²⁻ ions without the use of any template/capping agent (**S1-S3**). As mentioned before, the capping agents play an important role on the structure and properties of resulting nanostructures.²⁷⁻²⁹ In order to understand the effect of capping agent on the formation and the photocatalytic activity of CdS microspheres, we have also prepared mercaptoethanol (MCE) capped CdS microspheres (**S4**). Photocatalytic investigation of both uncapped (**S3**) and MCE-capped (**S4**) CdS microspheres for degradation of

MO under both UV and natural sunlight irradiation revealed higher photocatalytic activity of **S3** compared to that of **S4**. The relatively lower photocatalytic activity of **S4** has been attributed due to the effect of MCE capping agents which acts as a barrier for the interaction of MO molecules with the CdS nanocrystals. The syntheses procedure followed here is quite unique, it does not require the use of noxious sulfide sources and it can be carried out in air with high yield and almost uniform morphology of CdS microspheres.

2. Experimental

All the starting materials were commercially available and used as received without further purification. $\text{Cd}(\text{NO}_3)_2 \cdot 4\text{H}_2\text{O}$ and 4,4'-Dipyridyl disulphide (DPDS) were purchased from Sigma–Aldrich Chemical co. Methyl orange (MO) was purchased from Alfa Aesar. Dimethylformamide (DMF) and Ethanol were purchased from Merck and used as received.

2.1 Syntheses of CdS microspheres

The CdS microspheres (**S1–S4**) were synthesized using solvothermal method. To a DMF (2ml) solution of $\text{Cd}(\text{NO}_3)_2 \cdot 4\text{H}_2\text{O}$ (0.061 g, 0.2 mmol), ethanolic solution (1ml) of DPDS (0.044 g, 0.2 mmol) was added. The mixture with the solvent ratio 2:1 was stirred for 15 min and then taken in a 23 mL PTFE lined acid digestion bomb and heated at 120°C for 12h. After being cooled to room temperature the product was filtered and washed with ethanol few times and dried under vacuum. Greenish-yellow powder of CdS microspheres, **S1** has been isolated (yield: 85%). The CdS microspheres, **S2** and **S3** were prepared by following the similar procedure, except that the reaction temperature was maintained at 130°C and 140°C, respectively (yield: 82% (**S2**), 80% (**S3**)). The MCE-capped CdS microspheres, **S4** was prepared similar to that of **S3**, (at 140°C) except that, the synthesis was carried out in the presence of 5 equivalents (1 mmol, 70.13 μL) of mercaptoethanol (yield:84%).

2.2 Characterization

The powder X-ray diffraction (XRD) patterns were recorded on a PANalytical's X'PERT PRO diffractometer. Scanning electron microscopy (SEM) images were recorded using JEOL JSM-6610LV SEM with Energy Dispersive Spectroscopy (EDS) facility. Field-emission SEM (FESEM) images were recorded on a Carl zeiss ultra 55 FE SEM. Transmission electron microscopy (TEM), high-resolution TEM (HRTEM) and selected area electron diffraction (SAED) measurements were recorded using JEOL JEM-2100F Field Emission TEM. UV–vis spectra were recorded on a Perkin Elmer Model Lambda 900 spectrophotometer.

Thermogravimetric analyses (TGA) of the samples were carried out on Mettler Toledo TGA850 instrument. Fourier-transform infrared (FT-IR) measurements were recorded on Bruker TENSOR-27 spectrometer.

2.3 Photocatalytic tests

The photocatalytic activity of the CdS microspheres for the photocatalytic degradation of an aqueous solution of MO was carried out as follows: the as-prepared sample of CdS microsphere (S3/S4) (15 mg) was suspended in a solution of MO (5.0×10^{-5} M in 50 mL H₂O) in a beaker at ambient temperature. A 400 W high pressure mercury lamp was used as the UV-vis light source. The lamp was equipped with double walled quartz for constant water circulation which acts as a water filter to remove the heating effects. The setup was kept in the laboratory constructed irradiation box which has opening from top side. The distance between the UV light source and the beaker was maintained at 13 cm. Before irradiation, the suspension was stirred well in the dark for 30 minutes to establish an adsorption–desorption equilibrium between the CdS microspheres and MO then the photocatalytic reaction was initiated. The reaction was started after the intensity of the mercury lamp became stable. At regular time intervals, aliquots of the sample were withdrawn and the catalyst was separated through centrifugation and analyzed for MO dye concentration. The same experiment was repeated for the sample S3/S4 under sunlight on a clear day. The experiment was performed during the time interval of 10:30 am to 12 noon. The setup was kept in a place where the mixture was exposed to direct sunlight. The percentage degradation of MO dye was determined using the following relation.³⁰

$$\% \text{ Degradation} = \frac{C_i - C_f}{C_i} \times 100$$

Where, C_i and C_f are the initial and final concentrations of MO, respectively.

3. Results and Discussion

3.1 Characterization

The CdS microspheres, S1-S4 composed of CdS nanocrystals were synthesized by solvothermal route. The XRD patterns of the as-prepared samples of CdS microspheres, S1-S4 are shown in Fig. 1. The diffraction peaks are observed at $2\theta = 26.48^\circ$, 43.98° and 51.92° which are assigned due to (111), (220), and (311) planes of cubic or ZB structure of CdS (JCPDS reference code:10-454). The broadness of the diffraction peaks indicate the finite size of these crystallites. No additional diffraction peaks corresponding to either Cd(NO₃)₂ or any other

impurities were detected suggesting the purity of the materials. The calculated value of the mean crystallite size (D) using the Debye-Scherrer equation, $D = 0.94\lambda/B \cos\theta$ (where, D = crystallite size, λ = wavelength of X-ray (1.540598 Å), B = value of full width at half maximum (FWHM) and θ is the Bragg's angle) are 2.22, 2.40, 2.47 and 2.00 nm for **S1**, **S2**, **S3** and **S4** respectively.

The composition of the as-prepared samples (**S1-S4**) was determined by energy dispersive X-ray spectroscopy (EDX). As shown in Fig. 1b only peaks due to Cd^{2+} and S^{2-} were observed for uncapped sample **S3**. While the MCE-capped sample, **S4** shows additional peaks due to oxygen and carbon atoms of MCE capping agent (Fig. 1b). The quantitative analyses confirmed the atom ratio of $\text{Cd}^{2+}/\text{S}^{2-}$ to be 1:1. Also, the elemental mapping confirmed the homogeneous distribution of Cd^{2+} and S^{2-} elements in the CdS microsphere of **1** and **2** (Fig.2). Furthermore, FT-IR spectra of the samples **S1-S3** show only stretching bands due to solvent molecules (DMF and H_2O) and that of **S4** shows additional stretching bands at 2928, 2540, 1104, 1017, 695 cm^{-1} corresponding to C-H, S-H, C-O, C-C, and C-S stretching frequencies of MCE capping agent, respectively (Figs. S1 and S2, ESI). Therefore, the above mentioned analyses confirmed the formation of CdS microspheres without (**S3**) and with MCE-capping agent (**S4**).

The morphology of the as-prepared samples **S1-S4** was examined by SEM and TEM analyses. As shown in Fig.3 the SEM images of all the four samples show the presence of almost uniform solid spheres with diameters in the broad range of 0.5 to 2.5 μm (Fig. 3). The broad size distribution of CdS microspheres is due to self-agglomeration of nanocrystals. Therefore, the SEM images show the size of agglomerates of CdS nanocrystals and not the crystallite size. However, FESEM image of the CdS microspheres, **S3** and **S4** unveiled the presence of nanocrystals (Fig.4). Furthermore, the precise value of the crystallite's size was determined using TEM analyses. Fig. 5 shows low-magnification bright-field TEM image of a single CdS microsphere, of **S3** whose size is about 200 nm. Furthermore, the TEM image of a selected region on the surface of the microsphere shows the presence of CdS nanocrystals whose crystallite size lie in the range of 2-6 nm (insets of Fig. 5a), which is in near agreement with the crystallite's size value calculated from XRD (ca. 2.2 nm). The diffraction planes obtained from the SAED pattern match well with the XRD patterns and the HRTEM image shows structurally uniform lattice fringes of CdS nanocrystals, suggesting crystalline nature of the CdS material (Figs. 5b and c). The calculated fringe spacing of 0.34 nm corresponds to the (111) lattice plane of the cubic CdS. Fig. 6 shows low-magnification bright-field TEM image of MCE-capped CdS

microspheres, **S4**, with a size distribution of about 1.5-2 μm . The TEM image of a selected region on the surface of the microsphere shows the presence of ultra-small CdS nanocrystals whose crystallite's size lie in the range of 2-5 nm (inset (a) of Fig. 6), which is in near agreement with the value of crystallite size calculated from XRD (ca. 2.0 nm). The diffraction planes obtained from the SAED pattern match with the XRD patterns and the HRTEM image shows structurally uniform lattice fringes of CdS nanocrystals, suggesting crystalline nature of the CdS material (inset (b) and (c) of Fig. 6). The calculated fringe spacing of 0.35 nm corresponds to the (111) lattice plane of the cubic CdS. Hence, the above mentioned data clearly supports the formation of CdS microspheres composed of CdS nanocrystals.

3.2 Formation Mechanism of CdS Microspheres

The formation of CdS microspheres can be explained as shown in scheme 1. In situ generation of S^{2-} ions by the S-S bond cleavage of DPDS linker at temperatures above 120°C , followed by reaction with Cd^{2+} ions to form CdS nanocrystals. The self-aggregation of these nanocrystals to form CdS microspheres as depicted in Scheme 1. Here, DPDS molecule acts as a clean source of S^{2-} ions which are released in a controlled fashion by in situ S-S bond cleavage. Therefore, the formation of CdS microspheres, **S1-S4** can be explained by considering self-aggregation of individual CdS nanocrystals due to surface energy minimization as shown in Scheme 1.³¹

3.3 Optical properties

The room temperature UV-vis absorption spectra of CdS microspheres **S1-S4** dispersed in DMF is shown in Fig. 7. The spectra show sharp band edge absorptions in the visible-light region with a well defined absorption feature with absorption maximum at 444, 450, 435 and 347 nm, for **S1**, **S2**, **S3**, and **S4**, respectively. The blue shift in the absorption edge of the samples, in comparison with that of bulk CdS (515 nm) can be attributed due to quantum confinement effect.³² Similar observation of blue-shift in the absorption edge has been reported for CdS microspheres, suggesting that the UV-vis absorption mainly depends on the size of the primary particles and the hierarchical CdS microspheres exhibit the activity of their nanoscale building blocks.³³ The values of direct band gap energy (E_g) for the CdS microspheres was estimated from a plot of $(\alpha h\nu)^2$ versus photon energy ($h\nu$) using the relationship: $\alpha h\nu = A(h\nu - E_g)^n$ where, $h\nu$ = photon energy, A = constant, α = absorption coefficient, $\alpha = 4\pi k/\lambda$; k is the absorption index, λ is the wavelength, $n = 1/2$ for the allowed direct band gap.³⁴ The direct band gap values estimated

by extrapolating the absorption edge by a linear fitting method were 3.55, 2.93, 3.23 and 2.83 eV for sample **S1**, **S2**, **S3** and **S4**, respectively (See Figs. S3-S6, ESI).

3.4 Photocatalytic activity

In order to determine the potential applications of as-prepared CdS microspheres we investigated their photocatalytic activity for degradation of MO in aqueous solution under UV and natural sunlight irradiation. To eliminate the possibility of decoloration triggered by UV/sunlight, blank experiments were performed in the absence of the catalyst which showed negligible degradation of MO indicating the necessity of catalyst for the degradation process. Figs. 8a and b show the changes in the optical absorption spectra of MO at different time intervals under UV light irradiation catalyzed by CdS microspheres, **S3**. As the irradiation time increases the concentration of the MO decreases, at the end of 160 min the % degradation of MO was found to be 90.55% and 75.66% catalyzed by un-capped (**S3**) and MCE-capped (**S4**) CdS microspheres, respectively, (Figs. 8c and d) suggests higher photocatalytic performance of **S3** over **S4**.

Similar reactivity trend has been observed for the photocatalytic degradation of MO carried out under natural sunlight irradiation. As shown in the Figs. 9(a) and (b), at the end of 30 min the % degradation of MO catalyzed by **S3** and **S4** are 86% and 40%, respectively, indicating faster catalytic degradation under natural sunlight compared to those of UV light irradiation.

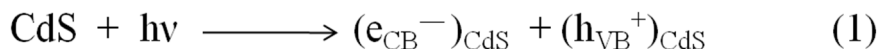
The kinetics of photocatalytic degradation of organic pollutants using semiconducting materials can be best described by pseudo first order reaction, $\ln(C_0/C_t) = k_{app}t$ (Where, C_0 is the concentration of the dye after adsorption in darkness for 30 min, and C_t is the concentration of the dye at given interval of time t). The plot of $\ln(C_0/C_t)$ vs t (Figs. 8(d) and 9(d)) represents a straight line and the slope of which upon linear regression equals first order rate constant k_{app} .³⁵ The calculated values of k_{app} for photodegradation of MO catalyzed by **S3** and **S4** under UV and natural sunlight irradiation are listed in the table 1. From the k_{app} values it is obvious that the catalytic activity of **S3** is much higher than that of **S4** under both UV light and natural sunlight irradiation. This difference in the photocatalytic activity can be ascribed due to the presence of capping agents in case of sample **S4** which interfere with the interaction of MO molecules with the CdS nanocrystals resulting in lower activity compared to uncapped CdS microspheres, **S3**.

S No	Catalyst and light source	Overall rate of the reaction (m ⁻¹)
1	S3, sunlight	7.1 x 10 ⁻²
2	S3, UV light	1.4 x 10 ⁻²
3	S4, sunlight	0.759 x 10 ⁻²
4	S4, UV light	0.725 x 10 ⁻²

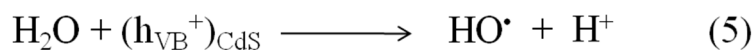
Table 1. The calculated values of rate constant (k_{app}) for photodegradation reaction of MO under UV and sunlight.

3. 5 Proposed mechanism for the degradation of the MO

The general mechanism of photocatalysis involves photoabsorption of a semiconducting material (SCM) leading to excitation of the electrons from the valence band (VB) to the conduction band (CB), to generate electron-hole (e_{CB^-}/h_{VB^+}) pair (eq 1).³⁶



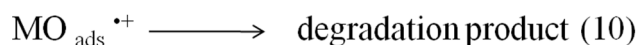
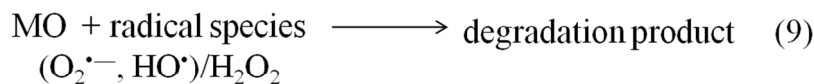
Then the photogenerated electron-hole pair migrates to the surface of the catalyst (CdS) and react with the adsorbed species on the surface (eqs 2-5). The transfer of the photogenerated electrons to the other species is crucial as it inhibits the recombination of the electrons and the holes hence increasing the activity of the photocatalyst.



As mentioned above the rate of photocatalytic degradation of MO is higher under natural sunlight irradiation compared to that of UV light irradiation (Table 1). This higher catalytic rate

can be attributed considering the operation of a dye sensitized photocatalytic process. In this case the MO dye molecules are excited by the visible light and they act as photosensitizers.³⁷⁻³⁸

Thus the reactive species ($O_2^{\bullet-}$, $\cdot OH$) produced as shown in the eqs 2-5 can then react with MO to form the degradation products via several possible pathways as has been proposed before (eqs 9-10) see ESI).³⁹⁻⁴¹



The observed difference in the photocatalytic activity of uncapped, **S3** and MCE-capped, **S4** microspheres can be explained as follows. The CdS nanocrystals in both **S3** and **S4** are quite active and can produce the electron-hole pairs under UV/sun light irradiation but their contact with air is obstructed by the presence of MCE-capping agents in case of **S4**. The MCE capping agents acts as a physical barrier and restricts the free access of MO molecules to catalytically active CdS nanocrystals in **S4**. Whereas, in the case of uncapped sample, **S3** the MO molecules can easily access to the surface of CdS nanocrystals and can interact with the charge carriers (electrons and holes) which is a crucial step in the degradation process. Therefore, in case of **S4** relatively less number of MO molecules are in contact with the surface of the CdS nanocrystals and resulting in lower catalytic efficiency.

It is worth mentioning that, the absorption edge of MO shows blue shift to shorter wavelength as shown in Fig 8b. This phenomenon indicates that MO molecules have been oxidized, and converted into smaller molecules with lower degree of π - π conjugation during the course of photocatalysis. The λ_{max} of the absorption spectra of these molecules produced during the degradation of MO is shorter than that of original MO molecules. Further oxidation gives rise to opening of aromatic rings leading consequently to degradation of MO to CO_2 and H_2O (Scheme S1, ESI).

4. Conclusions

A one pot solvothermal method for synthesizing template-free CdS microspheres composed of ultrasmall (~ 2 nm) CdS nanocrystals without (**S1-S3**) and with the use of MCE-capping agent (**S4**) has been developed. 4,4'-dipyridyldisulfide (DPDS) has been found to be a very useful temperature controlled in situ source of S^{2-} ions for the formation of CdS nanocrystals. A

possible mechanism has also been proposed wherein self-aggregation of individual CdS nanocrystals led to the formation of microspheres. Photocatalytic investigation of both uncapped (**S3**) and MCE-capped (**S4**) CdS microspheres revealed very good photocatalytic activity for degradation of MO under UV and natural sunlight irradiation. It is interesting to note that the photocatalytic activity of uncapped CdS microspheres is much higher than that of MCE-capped CdS microspheres. Thus the influence of capping agent on the photocatalytic performance of CdS microspheres under UV and natural sunlight irradiation has been studied. The difference in the photocatalytic performance has been attributed due to the presence of capping agents in **S4** which acts as a barrier for the interaction of MO molecules with the CdS nanocrystals. The excellent photocatalytic activity of **S3** under natural sunlight implies its potential application in the degradation of the dyes especially in water purification technology.

ACKNOWLEDGMENT

CMN gratefully acknowledges the financial support from the Department of Science and Technology (DST), Government of India (Fast Track Proposal). Thanks are also due to Prof. M. K. Surappa, director IIT Ropar for his encouragement.

References

1. A. P. Alivisatos, *Science.*, 1996, **271**, 933-937.
2. M. A. El-Sayed, *Acc. Chem. Res.*, 2004, **37**, 326.
3. M. J. Bowers II, J. R. McBride, and S. J. Rosenthal, *J. Am. Chem. Soc.*, 2005, **127**, 15378.
4. X. Chen, A. C. Samia, Y. Lou, and C. Burda, *J. Am. Chem. Soc.*, 2005, **127**, 4372.
5. R. Jose, N. U. Zhanpeisov, Y. B. Hiroshi Fukumura, and M. Ishikawa, *J. Am. Chem. Soc.*, 2006, **128**, 629.
6. S. Sapra, S. Mayilo, T. A. Klar, A. L. Rogach, and J. Feldmann, *Adv. Mater.*, 2007, **19**, 569.
7. R. Jose, Z. Zhelev, R. Bakalova, Y. Baba, and M. Ishikawa, *Appl. Phys. Lett.*, 2006, **89**, 013115.
8. A. Nag and D. D. Sarma, *J. Phys. Chem. C*, 2007., **111**, 13641.

9. A. Puzder, A. Williamson, F. Gygi, and G. Galli, *Phys. Rev. Lett.*, 2004, **92**, 217401.
10. J. R. I. Lee, R. W. Meulenbergh, K. M. Hanif, H. Mattoussi, J. E. Klepeis, L. J. Terminello, and T. van Buuren, *Phys. Rev. Lett.*, 2007, **98**, 146803.
11. T.Y. Wei, C.T. Huang, B. J. Hansen, Y. F. Lin, L. J. Chen, S.Y. Lu and Z. L. Wang, *Appl. Phys. Lett.*, 2010, **96**, 13508.
12. A. K. Rath, S. Bhaumik and A. J. Pal, *Appl. Phys. Lett.*, 2010, **97**, 113502.
13. P. V. Kamat, *Acc. Chem. Res.*, 2012, **45**, 1906.
14. T. Zhai, X Fang, L Li, Y. Bando and D. Golberg., *Nanoscale.*, 2010, **2**, 168.
15. X. Li, Y. Xi, C, Hu and X. Wang, *Mat. Res. Bull.*, 2013, **48**, 295.
16. S. Rengaraj , S. Venkataraj, S. H. Jee, Y. Kim, C. W. Tai, E. Repo, A. Koistinen, A. Ferancova and M. Sillanpaa., *Langmuir.*, 2011, **27**, 352.
17. T. Zhai, X. Fang, Y. Bando, B. Dierre, B. Liu, H. Zeng, X. Xu, Y. Huang, X. Yuan, T. Sekiguchi, D. Golberg., *Adv. Funct. Mater.*, 2009, **19**, 2423.
18. N. Pinna, K. Weiss, H. S. Kongehl, W. Vogel, J. Urban and M. P. Pileni., *Langmuir*, 2001, **17**, 7982.
19. J. H. Warner, R. D. Tilley, *Adv. Mater.*, 2005, **17**, 2997.
20. F. Chen, R. Zhou, L. Yang, N. Liu, M. Wang and H. Chen, *J. Phys. Chem. C.*, 2008, **112**, 1001.
21. F. Gao, Q. Y. Lu, X. K. Meng and S. Komareni, *J. Phys. Chem. C.*, 2008 , **112**, 13359.
22. C. W. Ge, M. Xu, J. H. Fang, J. P. Lei, H. X. Ju, *J. Phys. Chem. C.*, 2008, **112**, 10602.
23. C. C. Kang, C. W. Lai, H. C. Peng, J. J. Shyue, P. T. Chou, *ACS Nano.*, 2008, **2**, 750.
24. M. Gea, Y. Cuib, L. Liua, Z. Zhou, *Appl. Sur. Sci.*, 2011, **257**, 6595.
25. C. Wei, W. Zang, J. Yin, Q. Lu, Q. Chen, R. Liu, F. Gao, *Chem Phys Chem.*, 2013, **14**, 591.
26. C. M. Nagaraja and M. Kaur, *Mat. Lett.*, 2013, **111**, 230.
27. N. Zhiqiang and L. Yadong, *Chem. Mater.*, 2014, **26**, 72.
28. N. C. Sagaya Selvam, J. J. Vijaya and L. J. Kennedy, *Ind. Eng. Chem. Res.*, 2012, **51**, 16333.
29. K. R. Kahsar, D. K. Schwartz and J. W. Medlin, *ACS Catal.*, 2013, **3**, 2041.
30. A. N. Okte and O. Yilmaz, *Appl. Catal. B. Environ.*, 2008, **85**, 92.
31. G. Lin, J. Zheng and R. Xu, *J. Phy. Chem. C.*, 2008, **112**, 7363.

32. H. Weller, *Angew. Chem. Int. Ed.*, 1993, **32**, 41.
33. Y. Xu, C. Song, Y. Sun and D. Wang, *Mat. Lett.*, 2011, **65**, 1762.
34. F. Yang, N. N. Yan, S. Huang, Q. Sun, L. Z. Zhang and Y. Yu, *J. Phys. Chem. C.*, 2012, **116**, 9078.
35. C. Dong, M. Zhong, T. Huang, M. Ma, D. Wortmann, M. Brajdic, and I. Kelbassa, *ACS Appl. Mater. Interfaces.*, 2011, **3**, 4332.
36. H. Zhang and Y. Zhu., *J. Phys. Chem. C.*, 2010, **114**, 5822.
37. H. Gülce, V. Eskizeybek, B. Haspulat, F. Sarı, A. Gülce, and Ahmet Avcı, *Ind. Eng. Chem. Res.*, 2013, **52**, 10924.
38. R. Vinu, S. Poliseti and G. Madras, *Chem. Eng. J.*, 2010, **165**, 784.
39. P. Raja, A. Bozzi, H. Mansilla, and J. Kiwi, *J. Photochem. Photobiol. A.*, 2005, **169**, 271.
40. M. Styliidi, D. I. Kondarides and X. E. Verykios, *Appl. Catal. B.*, 2004, **47**, 189.
41. A. H. Boonstra and C. A. H. A. Mutsaers, *J. Phys. Chem.*, 1975, **79**, 1940.

Figures with Caption

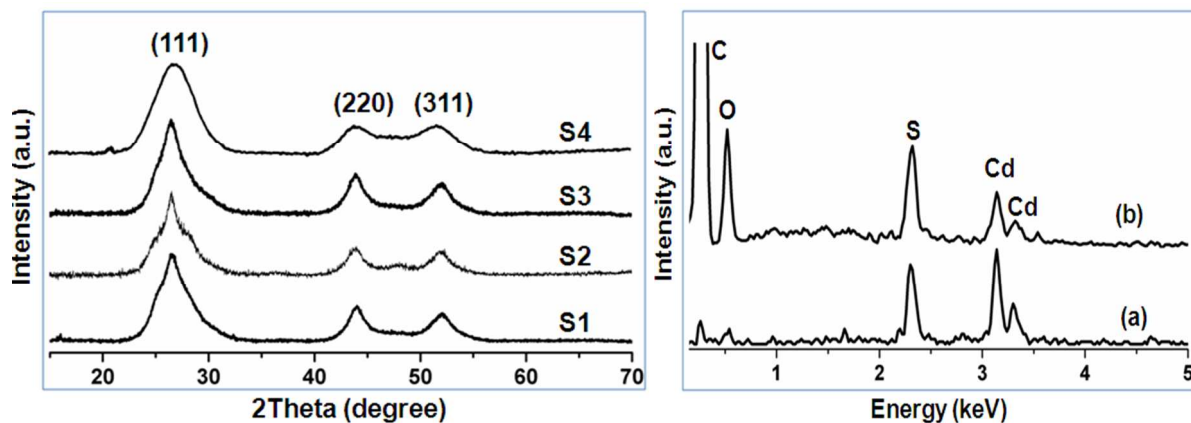


Fig. 1 (a) XRD patterns of the as-prepared CdS microspheres prepared at temperature of 120° (S1), 130° (S2), 140° (uncapped, S3) and 140°C (MCE-capped, S4). (b) EDS spectra of the as-prepared samples of S3 (a) and S4 (b).

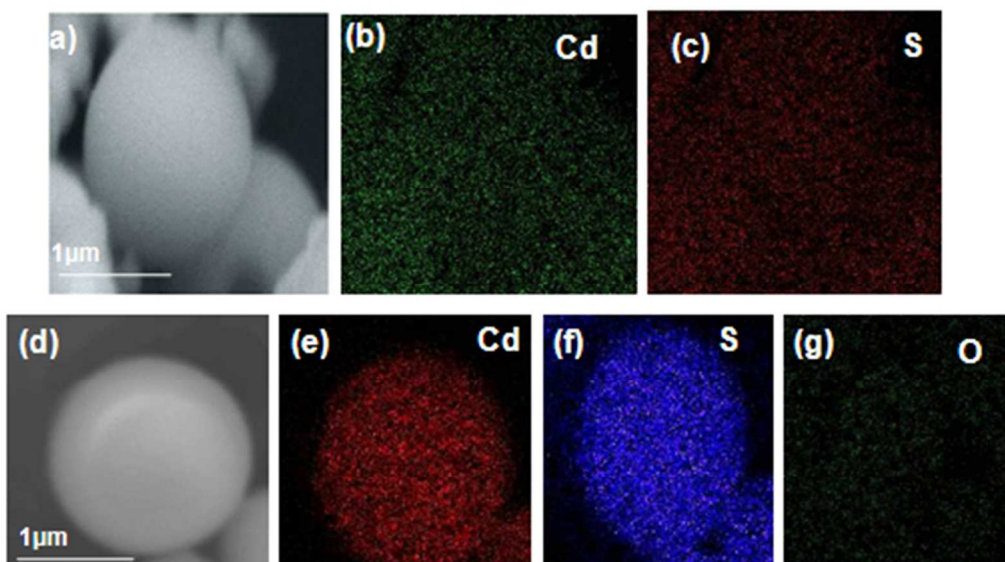


Fig. 2 EDX elemental mapping images for microsphere **1** (a-c) and **2** (d-g); the elemental mapping shows the homogeneous distribution of Cd and S elements in the CdS microsphere **1** and **2**.

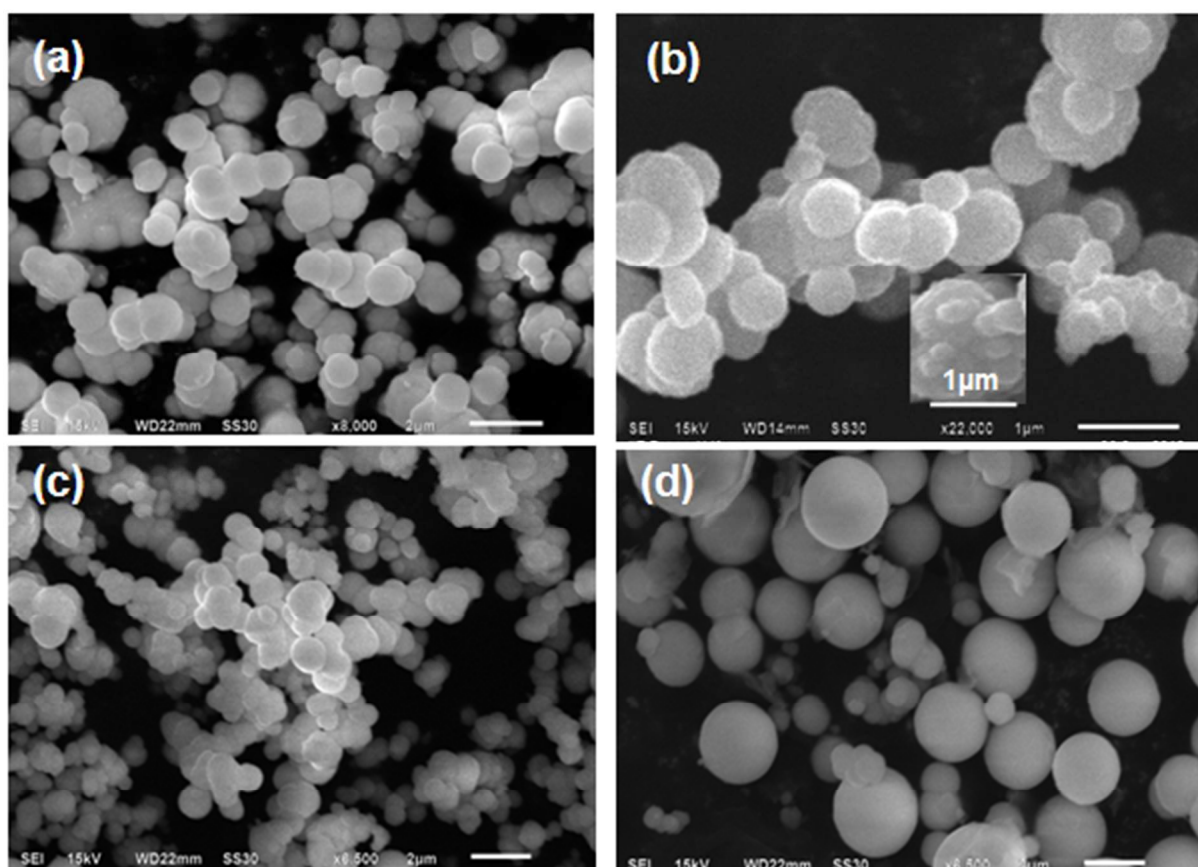


Fig. 3 SEM images of the as-prepared CdS microspheres prepared at (a) 120°C (S1), (b) 130°C (S2, inset shows magnified image of a microsphere showing the presence of CdS nanocrystals), (c) 140°C (S3) and (d) 140°C with MCE-capping agent (S4).

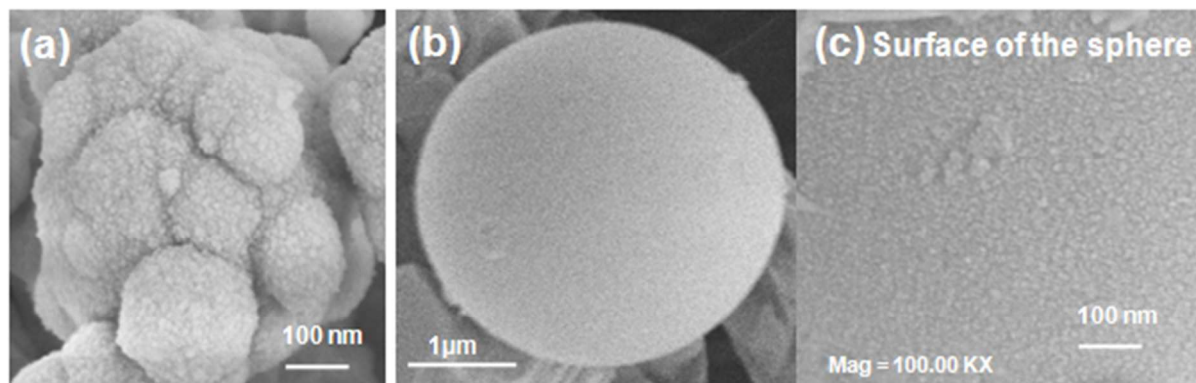


Fig. 4 FESEM images of a CdS microsphere, S3 (a) and S4 (b and c) showing the presence of nanocrystals.

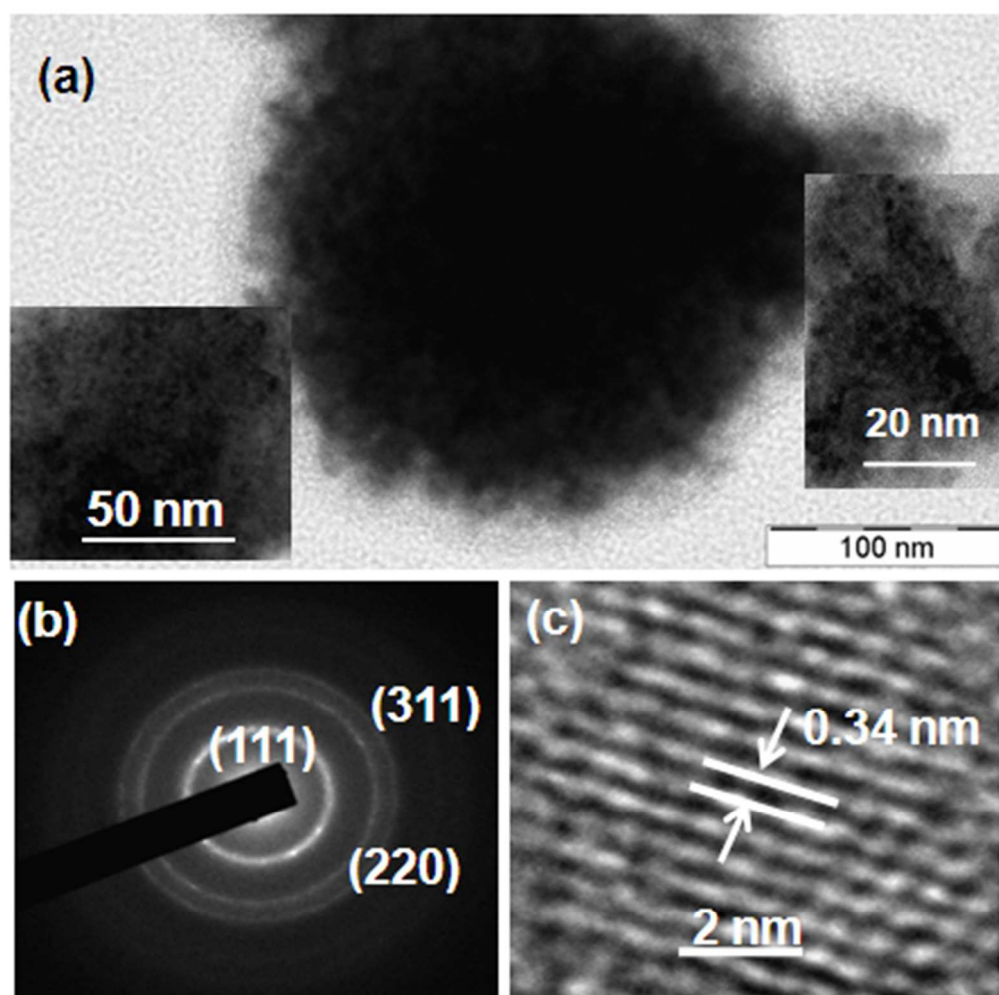


Fig. 5 (a) TEM image of the sample S3 showing the single CdS microsphere (insets: magnified images showing the presence of CdS nanocrystals), (b) and (c) shows the SAED pattern and the lattice fringe of CdS respectively.

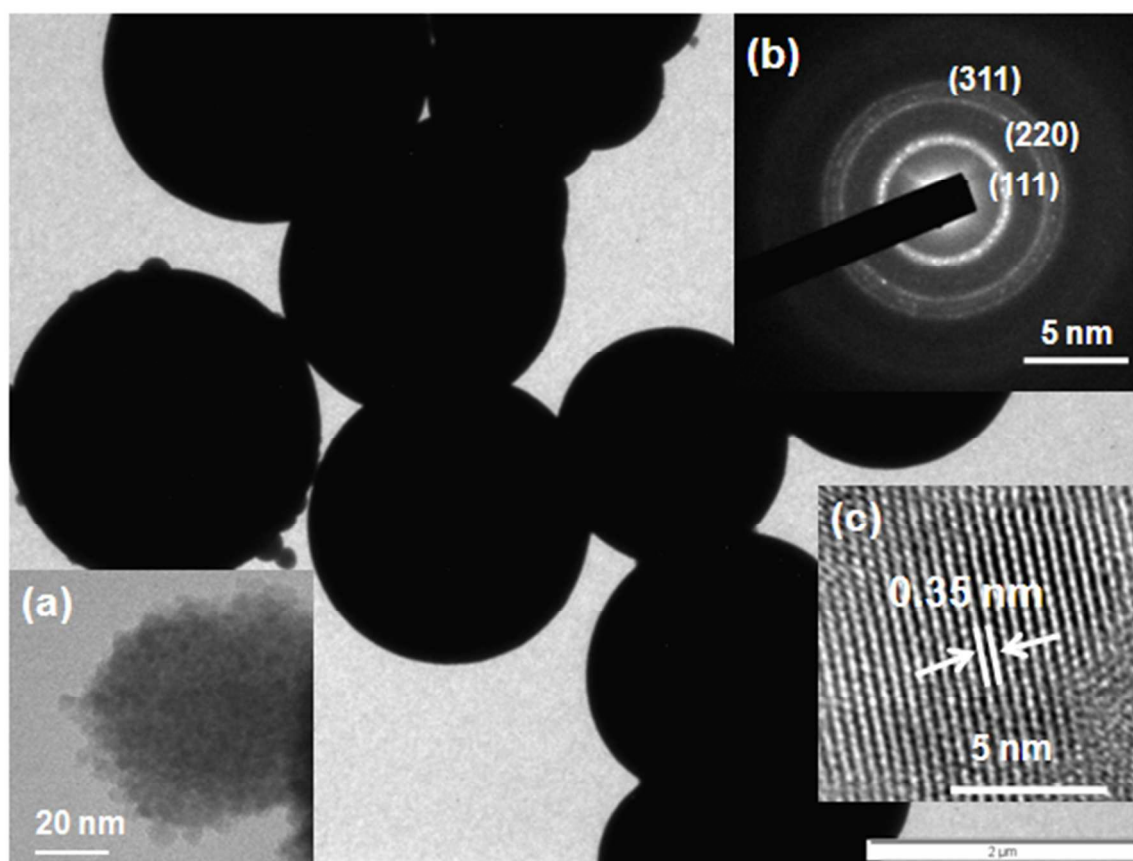
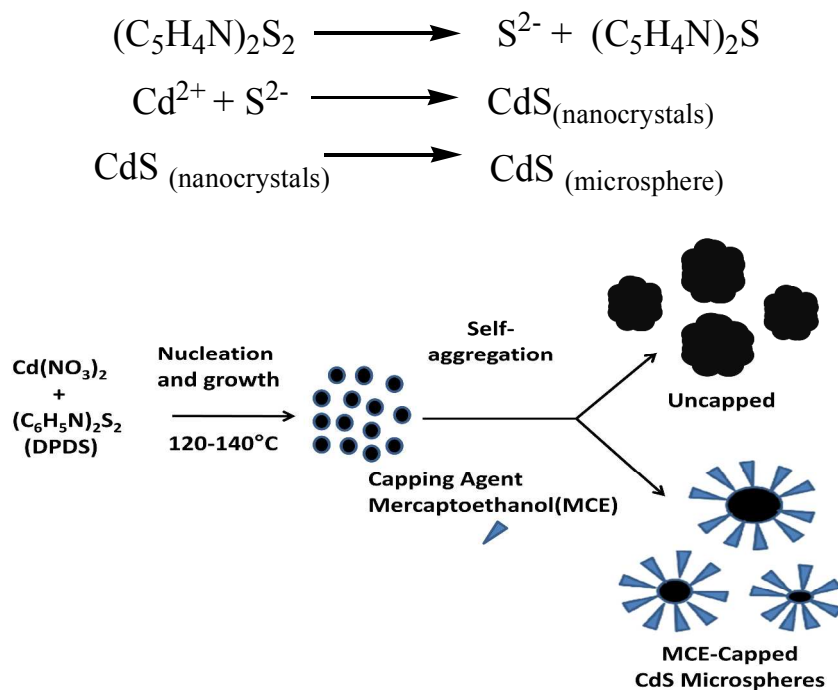


Fig. 6 (a) TEM image of MCE-capped CdS microspheres, S4 showing the CdS microspheres, inset (a) magnified image of a microsphere showing the presence of CdS nanocrystals, insets (b) and (c) show the SAED pattern and lattice fringe of CdS respectively.



Scheme 1. The proposed mechanism for the formation of CdS microspheres

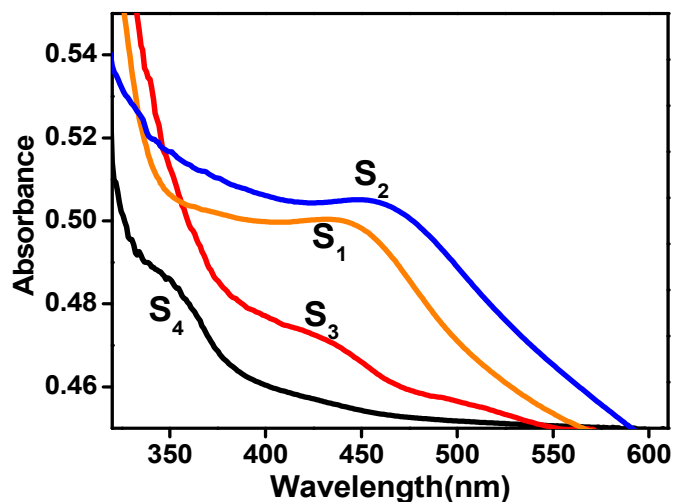


Fig. 7 (a) UV-vis absorption spectra of the CdS microspheres S1-S4.

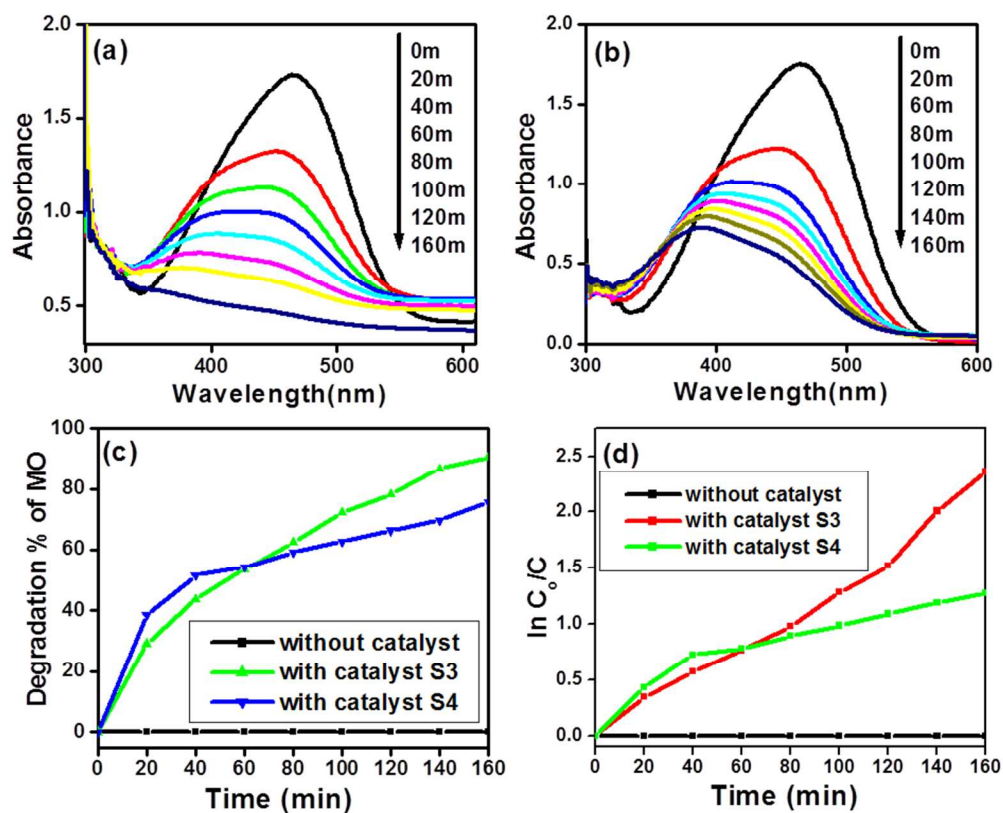


Fig.8 Time-dependent UV–vis absorption spectra for degradation of MO (5.0×10^{-5} M in 50 mL H_2O) using CdS (15 mg) microspheres (15 mg S3) (a) and S4 (b) under UV light, (c) percentage conversion of MO with time (d) plot of $\ln(C_0/C)$ with time.

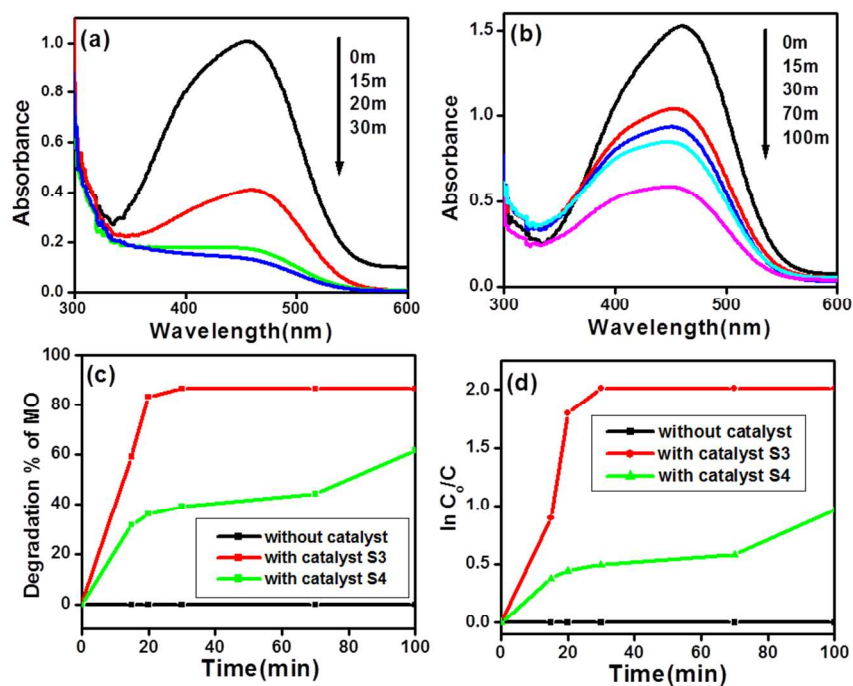


Fig. 9 Time-dependent UV-vis absorption spectral changes for aqueous MO solution catalyzed by CdS microspheres, S3 (a) and S4 (b) under natural sunlight; (c) percentage conversion of MO with time. (d) plot of $\ln(C_0/C)$ with time.

For graphical abstract

A one-pot, template-free, solvothermal method for synthesizing CdS microspheres composed of ultrasmall (~ 2 nm) nanocrystals using $(C_5H_4N)_2S_2$ as in situ source of S^{2-} ions without and with the use of MCE-capping agent has been developed. The photocatalytic activity of the microspheres for degradation of MO under UV and natural sunlight irradiation has been compared.

